The role of rare earth dopants in nanophase zirconia catalysts for automotive emission control

C.-K. Loong[a,*], M. Ozawa[b]

[a]*Argonne National Laboratory, Argonne, IL 60439-4814, USA*
[b]*Nagoya Institute of Technology, Tajimi 507-0071, Japan*

Abstract

Rare earth (RE) modification of automotive catalysts (e.g., ZrO_2) for exhaust gas treatment results in outstanding improvement of the structural stability, catalytic functions and resistance to sintering at high temperatures. Owing to the low redox potential of nonstoichiometric CeO_2, oxygen release and intake associated with the conversion between the 3+ and 4+ oxidation states of the Ce ions in Ce-doped ZrO_2 provide the oxygen storage capacity that is essentially to effective catalytic functions under dynamic air-to-fuel ratio cycling. Doping tripositive RE ions such as La and Nd in ZrO_2, on the other hand, introduces oxygen vacancies that affect the electronic and ionic conductivity. These effects, in conjunction with the nanostructure and surface reactivity of the fine powders, present a challenging problem in the development of better ZrO_2-containing three-way catalysts. We have carried out in situ small- to wide-angle neutron diffraction at high temperatures and under controlled atmospheres to study the structural phase transitions, sintering behavior, and $Ce^{3+} \leftrightarrow Ce^{4+}$ redox process. We found substantial effects due to RE doping on the nature of aggregation of nanoparticles, defect formation, crystal phase transformation, and metal–support interaction in ZrO_2 catalysts for automotive emission control. © 2000 Elsevier Science S.A. All rights reserved.

Keywords: Rare earth dopants; ZrO_2; Automotive exhaust; Emission control

1. Introduction: a new challenge in materials research for better autocatalysts

Concern regarding the grave consequences of excessive emission of greenhouse gases and other pollutants has risen to a global level with multiple impacts on modern societies. Automotive exhaust is identified as one of the major sources of air pollution. In response to popular awareness, governments, led by the United States, the European Community and Japan are imposing strict regulatory policies of standards on automotive emission. Current federal standards require a vehicle emission of hydrocarbon (HC)/CO/NO_x less than 0.31/4.2/0.6 g/mi with a durability of 100 000/10 mileage/year. In 2004 a more severe standard (0.125/1.7/0.2 g/mi) will be enforced. California State laws call for a more stringent control [1]. Although the three-way catalytic converter (TWCC) for automobiles was celebrated as one of the most successful anti-air pollution devices in the twentieth

century, the new requirement of the 'ultralow emission vehicles' will demand a performance level of the conventional TWCC going beyond its current capability. In addition, the imposition of limited CO_2 emissions requires a shift of the air-to-fuel ratio (A/F) to the 'lean-burn' condition, which the current TWCCs are unable to adequately remove the pollutants, particularly NO_x. Consequently, high-performance three-way catalysts (TWCs) for purification of automotive exhaust are in great demand. The development of durable, high-activity, and versatile TWCs has become a pressing issue in governmental and industrial research.

Common TWCs consist of precious metals (e.g., platinum, palladium and rhodium), supports (e.g., transition aluminas) and promoters (e.g., rare-earth oxides and zirconia). Cerium dioxide (CeO_2) is one of the most important promoters in TWC for its ability in enhancing the removal of carbon monoxide (CO), hydrocarbon (HC) and nitrogen oxide (NO_x) pollutants [2,3]. The oxide promoters of trivalent RE including La and Nd effect better NO_x–CO oxidation on precious metals. ZrO_2 stabilized by CeO_2 and other RE is know to increase durability and removal efficiency. Optimization of the parameters in the composition and structure of these oxides in conjunction with

---

*Corresponding author. Tel.: +1-630-252-5596; fax: +1-630-252-4163.

E-mail address: ckloong@anl.gov (C.-K. Loong)

application of precious metals has lead to the high performance of modern TWCs.

While traditional experimental methods, such as thermal analysis, temperature-programmed desorption measurements, microscopy and chemical probes, are useful, microscopic investigations at nanometer resolution of the structural and dynamic properties of catalysts in an environment that simulates operational conditions have become important. X-ray and neutron studies can in principle provide new information on several key issues, such as: (a) the microscopic structure of heterogeneous catalysts in terms of atomic positions and formation of vacancies or defects in non-stoichiometric and dopant-modified materials; (b) the surface chemistry involving the adsorption and desorption of molecules; (c) the kinetics of redox reactions of ceria in TWCs under dynamic A/F fluctuations; and (d) the evolution of microstructure (e.g., phase transformations, atomic diffusion, aggregate and sintering of particles, etc.) in practical catalysts during operation cycles. In this paper we report recent neutron studies of a series of rare-earth-doped zirconia TWCs, with emphasis on the role of rare-earth elements in promoting catalytic reactions through structural modification. The future trend of in situ scattering experiments using neutrons and X-rays for the characterization of rare-earth containing catalysts will also be discussed.

2. Effects of rare-earth (RE) doping on the microstructure of a powder

Control of the microstructure in powders (e.g., aggregation of crystallites, pore morphology) is one the important areas in materials research. Ultrafine zirconia powders are commonly prepared by hydrolysis of a zirconyl salt such as $ZrOCl \cdot 8H_2O$. The aqueous solution is treated by combined steps involving heating, aging, and pH control until a hydrous zirconia gel is produced either from precipitation or centrifugation [4]. The zirconia powder is obtained by filtering, washing and calcining the gel. Despite of numerous studies, the hydrolysis, complexation, and precipitation of the cationic species are not fully understood. It is thought that initially tetramers of $[Zr_4(OH)_8 \cdot 16(H_2O)]^{8+}$, each of which consists of a square planar array of four Zr cations bridged by OH ions and surrounded by H_2O molecules, are formed in the solution [5]. Under appropriate conditions upon heating or pH adjustment, the tetramers interact to form initially octamers and then higher-order complexes that may involve two-dimensional sheets before the eventual precipitation of three-dimensional structure [6]. Previous small-angle X-ray scattering (SAXS) provided evidence of the formation of tetramers, octamers and high-order complexes [7]. The rare-earth-modified zirconias of the present study were prepared by a coprecipitation technique from a $ZrOCl_2$ and $RECl_3$ solution [4]. Since RE differs from Zr in the ionic

size and/or charges, the microstructure of the RE-modified powder is expected to be different from that of pure zirconia.

Small-angle neutron scattering (SANS) enables the characterization of the microstructure in terms of primary-particle size, surface area, porosity, and nature of aggregation over a length scale of ~1–100 nm. Fig. 1 shows the SANS profiles (log–intensity versus log–Q, where Q is the neutron wavevector) of the 10 mol% RE-doped zirconia (RE=Ce and Nd) and the pure zirconia. All the powders were annealed at 600°C in air for ~3 h. The intensity profiles of the three samples show distinct Q-dependence, which indicates specific microstructural changes are introduced by each RE-dopant. The data (symbols) can be quantitatively analyzed by a mass-fractal model (solid curves) [8,9]. From a least-squares fit, the mean particle size of the Nd-doped, Ce-doped and pure zirconia are estimated to be 6.56, 20.6 and 22.8 nm, respectively. The particle-size distribution, in terms of the standard deviation of a log-normal distribution, are 1.17, 1.44 and 1.49, respectively. A standard deviation of unity implies a perfectly uniform size distribution (monodispersity). This result indicates that doping Nd(III) ions in ZrO_2 is more effective in preserving the small, relatively uniform particle size and the large surface area of the powder. This in part is due to the larger ionic radius of Nd^{3+} (0.112 nm) than that of Ce^{4+} (0.098 nm) and Zr^{4+} (0.084 nm) which hinders diffusion of atoms from sintering into larger particles. The slope of the curve over the Porod regime (the high-Q region indicated by the straight lines) provides a measure of the surface roughness of the constituent particles in an aggregate. A slope of -4 indicates smooth
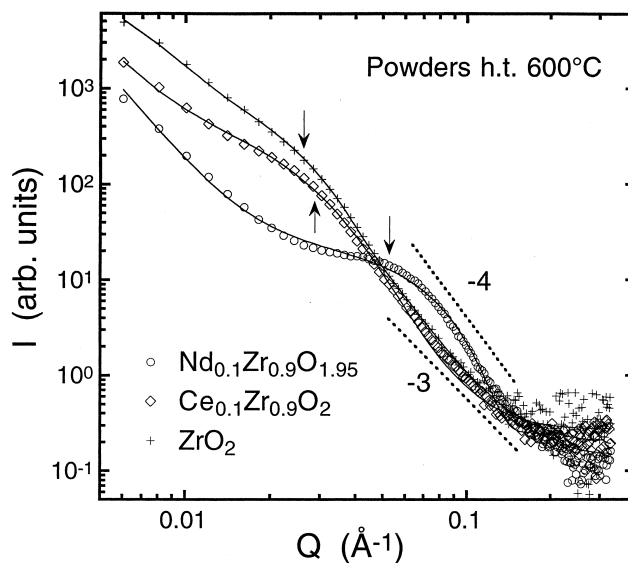

Fig. 1. The log–log plot of SANS intensity versus Q for $Nd_{0.1}Zr_{0.9}O_{1.95}$, $Ce_{0.1}Zr_{0.9}O_{1.95}$ and ZrO_2 that were heat-treated at 600°C. Typical errors are of the size of the symbols except for $Q>0.1$ Å^{-1} where errors are large. The solid lines represent the fits of the data to the fractal model. Limiting slopes for power-law behavior are given by the dotted lines.

surface and a value between -3 and -4 implies rough fractal-like surface. It can be seen from Fig. 1 that the slope for the pure zirconia sample is approaching -4. Therefore, without RE dopant, a pure zirconia powder is susceptible to sintering to form larger and smoother particles [10].

3. The crystal structure of nanophase $CeO_2 \cdot ZrO_2$ solid solutions

Pure ZrO_2 has three polymorphs: a cubic fluorite structure (space group $Fm3m$) above 2640 K, a tetragonal structure ($P4_2/nmc$) between 1400 and 2640 K, and a monoclinic structure ($P2_1/c$) below 1400 K. Our previous studies showed that a small amount of rare-earth solutes (e.g., ~10 mol% La, Ce, and Nd) in nanophase zirconia powders can stabilize the tetragonal and cubic phases over a wide range of temperatures [11]. We studied the crystal structures of $Ce_xZr_{1-x}O_2$ ($0 \leq x \leq 1.0$) that were prepared by the coprecipitation method. Fig. 2 shows the neutron powder diffraction profiles and the Rietveld refinements for $x=0.2$, 0.6 and 1.0. The structural refinements indicate that the $x=0.2$ sample is a solid solution containing a major tetragonal phase (~71 mol%) and a minor monoclinic phase (~29 mol%). The sample of pure ceria ($x=1.0$) shows a cubic fluorite phase. However, in the $0.2 < x < 0.8$ compositions, the diffraction peak profiles exhibit large intrinsic widths and an additional Lorentzian-like components which are characteristic of small crystalline grains and possibly defect structure. Preliminary Reitveld analysis indicates that the samples contain a mixture of major tetragonal and minor cubic and monoclinic phases. The lattice parameters (tetragonal phase) increase with increasing Ce concentration as expected from the larger Ce^{4+} ionic radius.

The crystal structures and phase transformations in the $CeO_2 \cdot ZrO_2$ binary system have been investigated by many workers [12–25]. However, we are not aware of any systematic study of the crystal phases of nanostructured $CeO_2 \cdot ZrO_2$ powders prepared by low-temperature methods. Yashima et al. [16,17] studied two types of $CeO_2 \cdot ZrO_2$ samples prepared by solid-state reaction: the oxygen-deficient samples obtained from quenching the specimens at 1760°C in water and the oxygen-restored samples obtained from annealing the quenched specimens in air at 627°C. They found the high-temperature cubic phase can be retained in the quenched, oxygen-deficient samples, whereas in the oxygen-restored samples the tetragonal phase is formed for 30–65 mol% CeO_2 composition and mixed tetragonal and cubic phases for 70–90 mol% CeO_2. Meriani and co-worker [23,24] observed a single-phase of tetragonal symmetry in non-quenching samples containing 40–60 mol% CeO_2 and mixed phases in both the low and high CeO_2-content samples. Although the different synthesis methods do not warrant a direct comparison of the
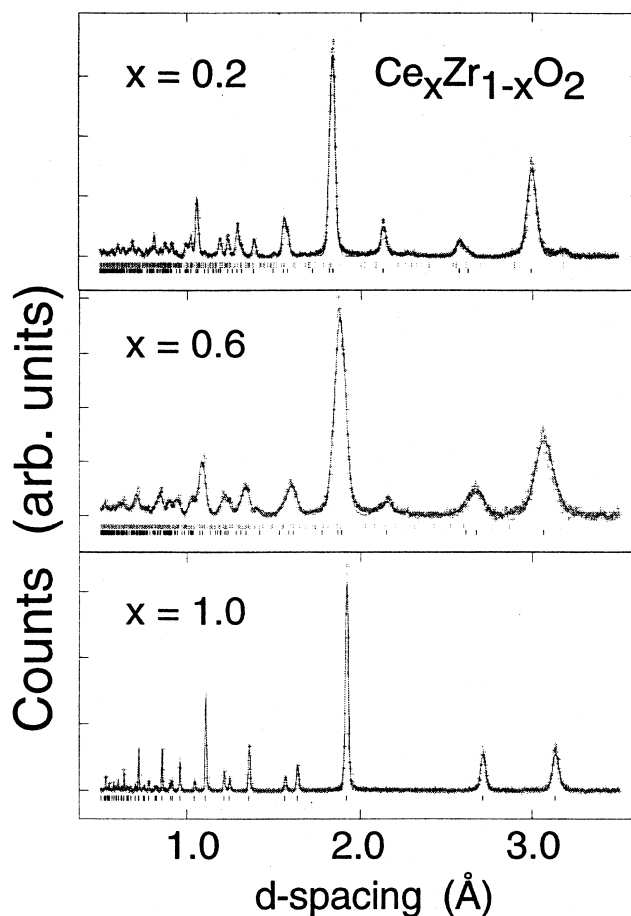

Fig. 2. Typical Rietveld profile fits in the 0.05–0.35 nm region of d-spacing for the $Ce_xZr_{1-x}O_2$ powders under a flowing 2% O_2/Ar gas environment at low temperatures (below 200°C). The symbols are the observed, background subtracted intensities. The solid line represents the calculated crystalline intensities. For the $x=0.2$ and 0.6 samples, the tick marks indicate the positions of the Bragg reflections of the monoclinic (top row) and tetragonal (bottom row) phases. CeO_2 ($x=1.0$) contains solely the cubic phase of fluorite structure.

crystal structures of the present samples with those found by other authors, accumulative evidence supports the formation of a predominant tetragonal phase of $Ce_xZr_{1-x}O_2$ for intermediate range of CeO_2 content. The detailed structural analysis of our samples over the entire composition range will be discussed in a later paper. Here we discuss the redox reactions in the $x=0.2$ (mainly tetragonal) and the $x=1.0$ (cubic) samples studied by in situ diffraction experiments.

4. The redox reaction of Ce ions in $CeO_2 \cdot ZrO_2$ three-way catalysts

Major pollutants (e.g, CO, HC, and NO_x) from automobiles are generated from incomplete combustion of gasoline and from the reaction of nitrogen with oxygen in the cylinder at combustion temperature. The chemical

reactions involved in the simultaneous reduction and oxidation of these pollutants during the catalyst operation are: $2CO+O_2 \rightarrow 2CO_2$, $2HC+3O_2 \rightarrow 2CO_2+H_2O$, $2CO+2NO \rightarrow 2CO_2+N_2$, $4HC+10NO \rightarrow 4CO_2+2H_2O+5N_2$. The success of the TWC relies on the control of the air-to-fuel mass ratio (A/F) to within a narrow window during the dynamic driving condition. This is achieved by the employment of oxygen sensors (which consist of rare-earth-doped zirconia electrolytes) in the exhaust stream in conjunction with a feedback control logic of the engine. However, a time lag between the sensor-signal processing and the A/F adjustment leads to an alternating (fuel) rich-lean deviation from the optimal stoichiometric A/F ratio. Owing to the low redox potential of non-stoichiometric CeO_2, oxygen release and intake resulting from conversion between the 3+ and 4+ oxidation states of the Ce ions in the oxide provide the oxygen storage capability (OSC) that are essential to the effective catalytic function under the fluctuating A/F environment.

It is well known that Ce^{4+} ions in $Ce_xZr_{1-x}O_2$ can be reduced to Ce^{3+} state, creating oxygen vacancies to form $Ce^{4+}_{x-2y}Ce^{3+}_{2y}Zr_{1-x}O_{2-y}$ [2]. However, in pure $CeO_2 \cdot ZrO_2$ the reduction occurs mainly on the surface region at high temperatures. For example, Zhu et al. [25] observed the phase separation in a 12 mol% CeO_2–ZrO_2 ceramic induced by $Ce^{4+} \rightarrow Ce^{3+}$ conversion at temperatures above 1000°C. In practice, however, the redox removal reaction can be facile if well-dispersed or high-surface area CeO_2–ZrO_2 complex oxides are used with Pt or Rh-based TWCs [26].

An understanding of the metal–support interactions in TWCs such as the $Ce_xZr_{1-x}O_{2-y}$/Pt system is paramount to the design and development of better air-pollution control catalysts. Harrison et al. [27] provided a model for the metal–ceria interaction during the oxidation of CO,

which is shown in Fig. 3. It involves the initial adsorption of CO molecules on Pt atoms and subsequently a reduction of Ce cations in the ceria/Pt interface. The $Ce^{4+} \rightarrow Ce^{3+}$ conversion releases oxygen atoms from ceria for the oxidation of CO to CO_2 which subsequently desorbs from the metal, leaving vacancies (denoted by dashed circles in Fig. 3) on the surface of the oxide particles. In order to sustain the redox reaction, the vacant sites have to be filled by oxygen from the lattice through atomic diffusion. Many aspects of the proposed mechanisms are still not understood. We are interested in the response to the redox process in the oxide lattice. Similar mechanisms for the redox reaction and oxygen-vacancy diffusion in $CeO_2 \cdot ZrO_2$ systems have been given by other workers [28].

Since neutrons probe the bulk of a sample rather than the surface, and the technique is sensitive to light atoms (e.g., O), it is useful to monitor the effects of oxygen or oxygen-vacancy diffusion on the structural modification under a typical catalytic operation such as redox reactions. This requires experiments undertaken in a sample environment that simulates the reaction chamber of practical OSC reactions. By virtue of the substantial difference in the ionic radius of Ce^{4+} (0.097 nm) and Ce^{3+} (0.114 nm), which permits the manifestation of the redox process via changes in the unit-cell volume of the lattice, we carried out in situ neutron diffraction on $Ce_xZr_{1-x}O_{2-y}$ with and without impregnated Pt (1 wt%) at high temperatures under oxidizing and reducing atmospheres. Diffraction data at each temperature were collected in the following manner for both samples: heating from 25 to 400°C in flowing $2\%O_2$ balanced by Ar gas followed by continued heating from 400 to 700°C in flowing 1% CO balanced by Ar. The temperature was stepped at an interval of 50°C and a 20-min wait prior to the 1-h data collection was allowed for thermal equilibration at each temperature. At selected
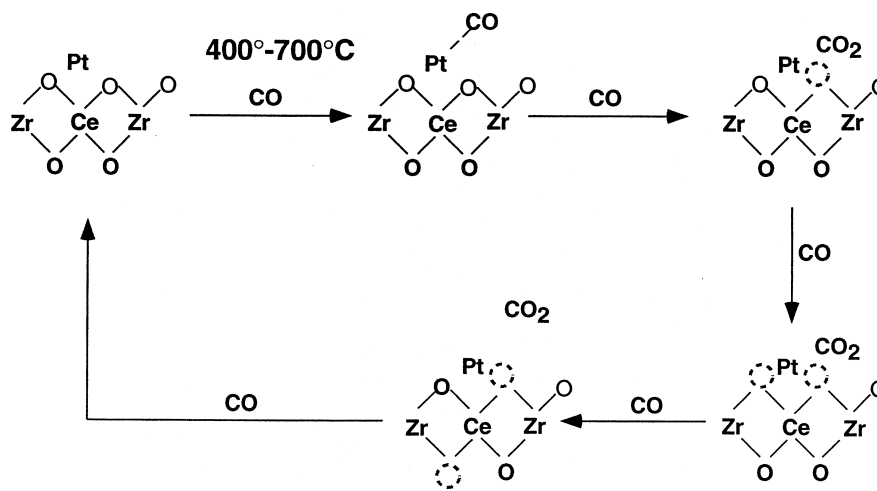

Fig. 3. A schematic model for oxidation of CO by a $CeO_2 \cdot ZrO_2$/Pt catalyst promoted by metal–oxide support interaction (after Ref. [27]). The dashed circles represent oxygen vacancies. A key step is the release of oxygen atoms in conjunction with the $Ce^{4+} \rightarrow Ce^{3+}$ conversion. Oxygen vacancies are generated initially at the ceria/Pt interface and subsequently migrate into the interior of the lattice.
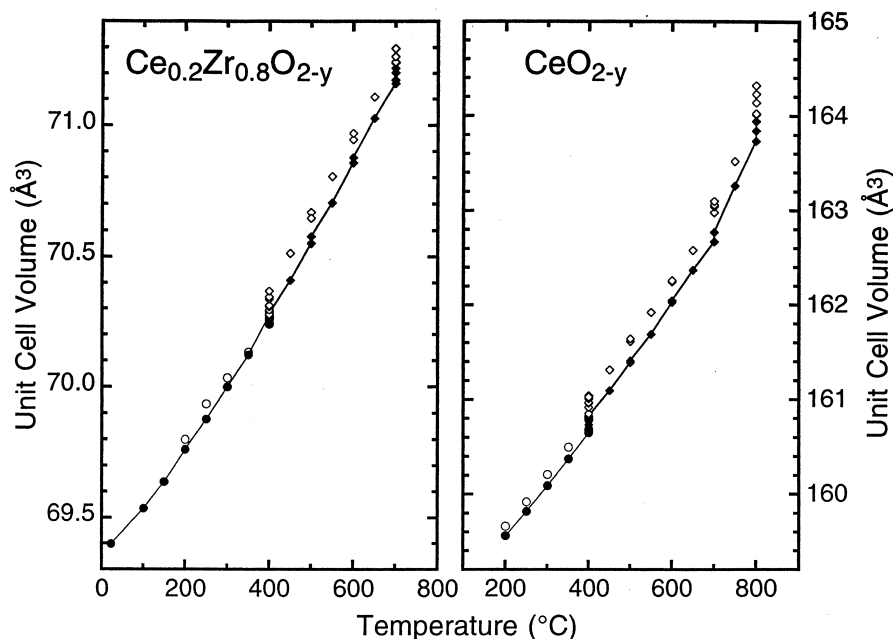
Fig. 4. The temperature and atmosphere dependence of the unit-cell volume of tetragonal $Ce_{0.2}Zr_{0.8}O_{2-y}$ (left) and CeO_{2-y} (right) with (open symbols) and without (solid symbols) Pt impregnation. The samples were first heated in 2% O_2/Ar (circles) and then switched to 1% CO/Ar and continued heating to 700 or 800°C (diamonds). Data were collected at each temperature for 1 h except at 400, 500, 600, 700 and 800°C multiple data sets were recorded every 0.5 h. Uncertainties of the data points are comparable to the size of the symbols.

temperatures between 400 and 800°C multiple 30-m data sets were collected. Fig. 4 shows the temperature and atmosphere dependence of the unit-cell volume of the tetragonal phase of $Ce_{0.2}Zr_{0.8}O_{2-y}$ and the cubic phase of CeO_{2-y} samples with and without dispersed Pt. First, under an oxidizing atmosphere (2% O_2/Ar) up to 400°C the lattice unit cell of the Pt-impregnated materials is slight larger than those without Pt. Second, as the gas is switched to a reducing atmosphere (1% CO/Ar), the lattice expands at a constant temperature, as can be seen from the multiple data points collected over 1–4-h periods at 400, 500, 600 and 800°C. Third, the expansion occurs at a much higher rate in the samples containing Pt. Similar phenomenon was also observed in other $Ce_xZr_{1-x}O_{2-y}$/Pt samples. The occurrence of anomalous thermal expansion only in a reducing atmosphere confirms the gradual conversion of the Ce^{4+} to larger Ce^{3+} ions. Since the observed d-spacing reflects the long-range order structure in the crystalline grains, the enhanced expansion in Pt-containing samples implies the migration of oxygen vacancies from the interfacial region between the oxide and Pt particles to the bulk of the oxide lattice. In samples contain no active metal component, on the other hand, the redox reaction and the generation of oxygen vacancies are limited mainly on the surface of the oxide grains. High activity requires heat treatments at higher temperatures (above ~700°C, see Fig. 4). Therefore, the neutron results support the model for metal–support interaction proposed by Harrison et al. [27].

5. Conclusion

We demonstrate the usefulness of a neutron-scattering method in the characterization of the structural modification of high-surface area zirconia powder by rare-earth doping. First, the growth of primary particles from hydrolysis or coprecipitation in $ZrOCl_2$ aqueous solutions, and the microstructural evolution due to annealing the obtained pure and R-modified ZrO_2 powders can be studied by small-angle scattering [10,29]. Second, through powder diffraction the formation of crystal phases depending on the composition in nanophase (coprecipitated) CeO_2–ZrO_2 as well as RE(III)-doped ZrO_2 can be characterized [11]. Third, the dynamics of hydrogen atoms associated with the surface hydroxyl groups and adsorbed water molecules on RE-modified ZrO_2 over a frequency range of 0–4400 cm^{-1} can be investigated by inelastic scattering. Details of these experiments are given elsewhere [30,31]. Finally, we emphasize the importance of in situ scattering experiments under controlled atmospheres and at high temperatures for the understanding of redox reaction involving Ce ions [32]. Here, we described the recent neutron-diffraction results concerning the crystal structures and the redox reaction in other compositions of CeO_2–ZrO_2. The present neutron-diffraction experiment was unable to determine quantitatively the fraction of $Ce^{3+} \leftrightarrow Ce^{4+}$ states during the measurement intervals. However, a recent in situ X-ray diffraction study using CO pulse reaction was successful in the characterization of the

reduction kinetics [33]. Currently, we continue our investigations over the full range of ceria composition in the $CeO_2 \cdot ZrO_2$ system, and extend the studies to zirconias prepared by sol–gel and microemulsion methods. Nanostructured zirconias prepared by these low-temperature processes can in principle provide much higher catalytic activity. In the climate of increasing public awareness and concern of environmental issues, the demand for better catalysts to cope with governmental regulations and industrial needs becomes imperative. Research of RE elements in catalytic applications by combining neutron scattering with other methods is expected to expand rapidly in the future.

Acknowledgements

References

[1] B.J. Cooper, Platinum Metals Rev. 38 (1994) 2.
[2] A. Trovarelli, Catal. Rev.-Sci. Eng. 38 (1996) 439.
[3] J. Barbier Jr., D. Duprez, Appl. Catal. B 4 (1994) 105.
[4] M. Ozawa, M. Kimura, J. Less-Common Metals 171 (1991) 195.
[5] C.F. Baes Jr., R.E. Mesmer, in: The Hydrolysis of Cations, Wiley, New York, 1976.
[6] A. Bleier andR, R.M. Cannon, Mater. Res. Soc. Symp. Proc. 73 (1986) 71.
[7] A. Singhal, L.M. Toth, J.S. Lin, K. Afholter, J. Am. Ceram. Soc. 118 (1996) 11529.
[8] S.K. Sinha, Physica D 38 (1989) 310.
[9] J. Teixeira, J. Appl. Crystallogr. 21 (1988) 781.
[10] C.-K. Loong, P. Thiyagarajan, J. Richardson, J.W.M. Ozawa, S. Suzuki, J. Catal. 171 (1997) 498.
[11] C.-K. Loong, J.W. Richardson Jr., M. Ozawa, J. Catal. 157 (1995) 636.
[12] E. Tani, M. Yoshimura, S. Somiya, J. Am. Ceram. Soc. 66 (1983) 506.
[13] E. Tani, M. Yoshimura, S. Somiya, J. Am. Ceram. Soc. 66 (1983) 11.
[14] P. Duwez, F. Odell, F.H. Brown Jr., J. Am. Ceram. Soc. 35 (1952) 107.
[15] M. Yashima, N. Ishizawa, M. Yoshimura, J. Am. Ceram. Soc. 75 (1992) 1550.
[16] M. Yashima, K. Morimoto, N. Ishizawa, M. Yoshimura, J. Am. Ceram. Soc. 76 (1993) 1745.
[17] M. Yashima, K. Morimoto, N. Ishizawa, M. Yoshimura, J. Am. Ceram. Soc. 76 (1993) 2865.
[18] M. Yashima, H. Arashi, M. Kakihana, M. Yoshimura, J. Am. Ceram. Soc. 77 (1994) 1067.
[19] M. Yashima, T. Mitsuhashi, H. Takashina, M. Kakihana, T. Ikegami, M. Yoshimura, J. Am. Ceram. Soc. 78 (1995) 2225.
[20] M. Yashima, S. Sasaki, Y. Yamaguchi, M. Kakihana, M. Yoshimura, T. Mori, Appl. Phys. Lett. 72 (1998) 182.
[21] S. Meriani, Thermo. Acta 58 (1982) 253.
[22] S. Meriani, Mater. Sci. Eng. 71 (1985) 369.
[23] S. Meriani, G. Spinolo, Powder Diffract. 2 (1987) 255.
[24] S. Meriani, Mater. Sci. Eng. A109 (1989) 121.
[25] H.-Y. Zhu, T. Hirata, Y. Muramatsu, J. Am. Ceram. Soc. 75 (1992) 2843.
[26] M. Ozawa, M. Kimura, A. Isogai, J. Alloys Comp. 193 (1993) 73.
[27] B. Harrison, A.F. Diwell, C. Hallett, Platinum Metals Rev. 32 (1988) 73.
[28] M.G. Sanchez, J.L. Gazquez, J. Catal. 104 (1987) 120.
[29] M. Ozawa, S. Suzuki, C.-K. Loong, P. Thiyagarajan, J. Mater. Sci. Lett. 16 (1997) 1360.
[30] C.-K. Loong, L.E. Iton, M. Ozawa, Physica B 213–214 (1995) 640.
[31] C.-K. Loong, F. Trouw, M. Ozawa, G. Zuzuki, in: P. Thiyagarajan, F. Trouw, C.-K. Loong, M.A. Marzec (Eds.), Materials Research Using Cold Neutrons at Pulsed Sources, World Scientific, Argonne National Laboratory, Argonne, IL, 1999, p. 185.
[32] C.-K. Loong, S.M. Short, M. Ozawa, S. Suzuki, Mater. Res. Soc. Symp. Proc. 497 (1998) 65.
[33] M. Ozawa, C.-K. Loong, Catal. Today 50 (1998) 329.